

# Tests of MVD Prototype pad detectors with a $\beta^-$ source

Sang Yeol Kim, Sang Su Ryu, Young Gook Kim  
Yonsei University  
John P. Sullivan  
Los Alamos National Lab

5 November 1997, draft 4

### **Abstract**

The Phenix MVD group has been testing two types of Si pad detectors for the “endcaps” of the MVD. One design, “single metal”, would require a more complex cable than the other design (“double metal”). We would prefer to use the double metal design, but there is some concern that this design will introduce crosstalk into the system. Therefore, a  $^{90}\text{Sr}$   $\beta^-$  source was used to measure the crosstalk in the system.

# 1 Introduction

The Phenix MVD group has been testing two types of Si pad detectors for the “endcaps” of the MVD. One design, “single metal”, has traces which take the signals from the pads (i.e. the keystone shaped counting elements which collect the charge) to the edges of the detector wafers. To prevent the traces from crossing, they are brought to 3 of the 4 edges of the detector wafer. These traces are in the same metallic plane as the pads. The signals would be connected to the electronics via relatively complex cable which overlays the detector wafer. The design of the cable is much simpler if a “double metal” detector design is used. In this design the traces which take the signals to the edge of the detector are separated from the pads by an oxide ( $\text{SiO}_2$ ) layer. The traces go from the pads, through the oxide layer, to a second “metal” layer. The signal traces can then all be brought to a single edge of the detector. This simplifies the cable design. However, there was some concern that the coupling through the capacitors formed by the traces from one pad crossing above the pads for other channels would introduce crosstalk into the system. In the study described here, we have measured the crosstalk in a prototype double metal pad detector.

A  $^{90}\text{Sr}$   $\beta^-$  source, used in various combinations with three trigger scintillators, was used to measure the crosstalk in the system.  $^{90}\text{Sr}$  decays to  $^{90}\text{Y}$  which then  $\beta$  decays. The beta decay spectrum from  $^{90}\text{Y}$  has an endpoint of 2.28 MeV. This is the electron used in the tests. A 2.28 MeV electron has a range in Si around 5mm ( $5000\mu\text{m}$ ). The thickness of the Si detector is  $300\mu\text{m}$ . So we could test the crosstalk in the double metal silicon pad detector using the beta source.

We established a limit on the amount of crosstalk which is acceptable by considering the effects of crosstalk of the pad detector trigger for central Au+Au events using a PISA simulation of the MVD with Hijing events as input. The average occupancy of the pad detector pads in this case was  $\approx 16\%$ . The discriminator thresholds on each pad, used in the trigger, will be set at about 0.25 times the average signal from a minimum-ionizing particle (mip). There are 21 pads in each “column” of pads. A column is a set of pads at the same azimuthal angle, but different radial distances from the beam. The signal traces in the double metal design all run to the top (largest radial distance from the beam) edge of the pad detector. This means that the top pad has 20 signal traces crossing it and that the bottom pad’s readout trace crosses over 20 other pads. If there is crosstalk between each pad in a column and the 20 other pads in the column, we would like the total crosstalk contribution to a pad without a hit to be small enough to avoid triggering the pad’s discriminator. That is we would like  $(\text{occupancy}=0.16) \times (20 \text{ pads in column contributing to crosstalk}) \times (\text{crosstalk}) \times (\text{average signal per particle}=1 \text{ mip})$  to be less than 0.25 mip. This gives a limit on the crosstalk of  $\text{crosstalk} < 0.25 / (20 * 0.16) = 7.8\%$ . Correction for crosstalk can be made, but we prefer to a level significantly below this limit.

## 2 General Setup

### 2.1 Cabling convention and FEE

The double metal silicon pad detector has 252 channels. It has 21 rows and 12 columns. The size of the readout pads is different row by row. Among the 252 channels we connected only 8 channels to the electronics because our test FEE board supports only 8 channels. Figure 1 shows the numbering of the channels used in this study. The readout pads for the three pads at the bottom(#1, #2, #3) are 2.0mm x 2.0mm which are the smallest among all the pad detector channels. Above them, pads #4, #5 are 2.5mm x 2.5 mm. The top most two channels(#7, #8)

have the largest channels have 4.5mm x 4.5 mm pads (the largest on the detector), and below them channel #6 has a 4.0mm x 4.0mm pad. Channel #1 through #5 are in the column neighboring the column containing channels #6 through #8. Therefore, the readout traces for channels 1–5 do not cross channels 6–8 and vice-versa. We used the a version of FEE which has the BVX pre-amplifier chip, and we wire bonded the 8 channels of silicon pad detector to the FEE.

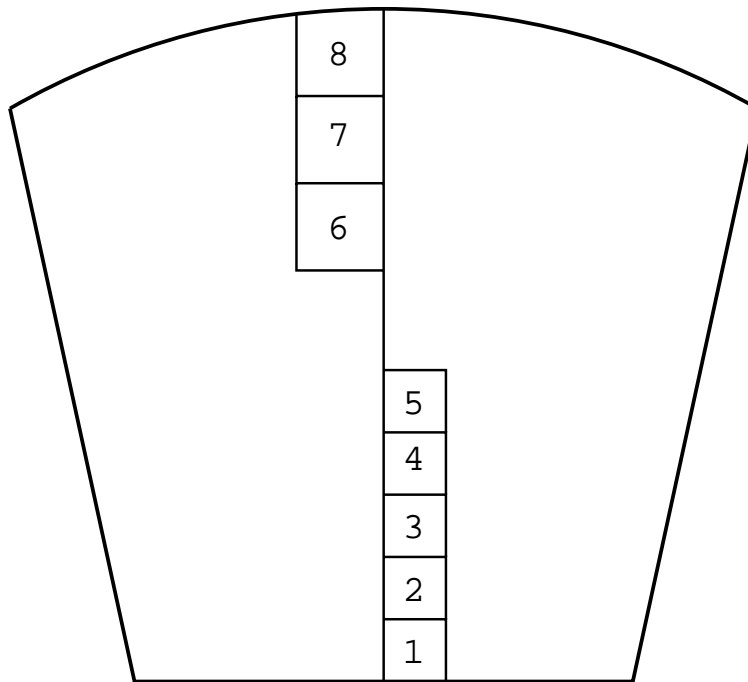


Figure 1: Cable labels.

## 2.2 Overall setup

The overall geometry of the test setup is shown in figure 2. We used three trigger scintillators in these tests. Two of the trigger scintillator scintillators used 2mm x 2mm x 25mm scintillating fibers which were configured in an “X” – when used in the trigger these two scintillators therefore defined a  $\approx 2\text{mm} \times 2\text{mm}$  square through which the electrons from the beta source passed. These two scintillators were used to define the incident angle of the beta particles. Beneath the crossed triggers counts there was a 25mm x 25mm x 12.5mm scintillation detector. This was used to cut the low energy beta particles. This was thick enough to stop all the beta particles from the  $^{90}\text{Sr}$  source. The silicon pad detector was placed 25mm above the upper most scintillation detector. The pad detector was supported by 2mm thick G10 circuit board, and the detector together with circuit board and FEE board were attached to the 15mm thick aluminium support. The higher energy electrons from the beta source have sufficient range to pass through the 300 $\mu\text{m}$  pad detector, the 2mm thick G10 circuit board, the two scintillating fibers, and then stop somewhere in the larger scintillator. However, the electrons can not penetrate the aluminium support, but a hole in the aluminium support allowed them to reach the scintillators. The source was positioned 20mm above the pad detector. There was no collimator except the hole on the brass source container.

All of the detectors and source assembly were placed in a dark box in order to prevent stray light from hitting the pad detector or scintillators. The FEE was inside the dark box, but the remaining electronics was outside. The electronics outside the dark box were composed of NIM amplifiers, discriminators, coincidence units, and CAMAC readout electronics. Because there was a DC component in the signal from the FEE, we used capacitors at the end of each channel's output from the FEE to get rid of the DC component. It is important to remember that we could not get a signal without this capacitor. (Some capacitor units actually contain an R-C circuit and will change the signal shape. So we think that we should use a capacitor without resistance.) We used a CAMAC system combined with VME to read out the data. A computer routine was written to control the CAMAC read out. It checks the LAM signal from one designated channel of ADC, and if LAM is on, it reads all the channels of ADCs. The details of the electronics set-up were different from test to test. The details of the different setups are given in the following sections which describe the individual tests.

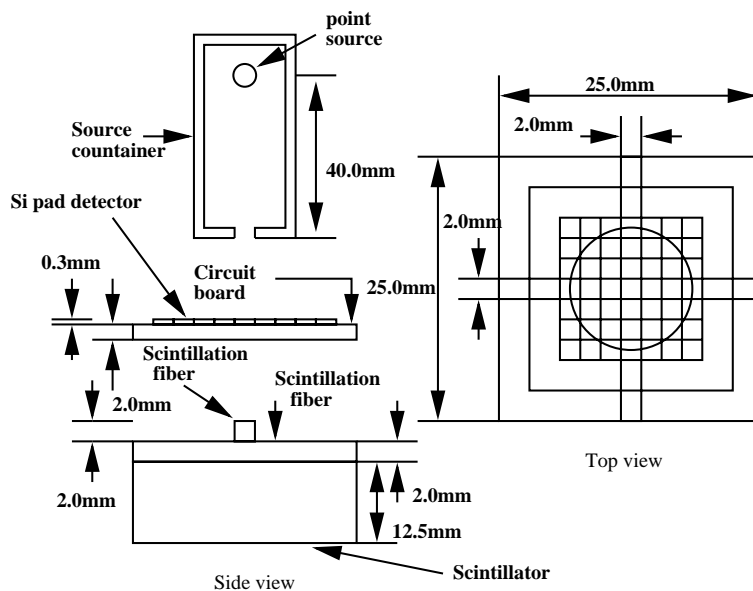


Figure 2: Detectors Geometry.

### 2.3 Source

We used  $^{90}\text{Sr}$  as a beta source for the crosstalk test.  $^{90}\text{Sr}$  has a half-life 28.74 years. It beta decays to  $^{90}\text{Y}$  with a 546.2keV beta end point energy.  $^{90}\text{Y}$  is also unstable and decays to  $^{90}\text{Zr}$  with a half-life 64.1 hours. All of the  $^{90}\text{Sr}$  decays to the ground state of  $^{90}\text{Y}$ .  $^{90}\text{Y}$  has a rather complicated decay scheme but most decays are to the ground state of  $^{90}\text{Zr}$  with a small branching ratio to an excited state which we can ignore. Figure 3 is the complete double decay scheme of  $^{90}\text{Sr}$ . The electrons actually in the crosstalk test are from the decays of  $^{90}\text{Y}$  to the ground state of  $^{90}\text{Zr}$  — which has its maximum beta energy 2281.4keV. The 64.1 hours half-life of  $^{90}\text{Y}$  is long enough to prevent accidental coincidences between beta particles from  $^{90}\text{Zr}$  and  $^{90}\text{Y}$ .

Using a Monte Carlo simulation, we checked that the higher energy electrons from  $^{90}\text{Y}$  can mimic the energy loss of a minimum-ionizing particle (mip). It can also penetrate all the elements

which compose of the silicon pad detector itself, its support structure, and all of the trigger scintillators. Although the beta endpoint energy is large enough to penetrate all detectors, the energy is low enough to allow many beta particles to deflect at large angles. The result is a severe loss of counting efficiency as can be seen in the table 2 in section 3.2. The dimensions of the source are shown in the figure 4. The source was a point source contained inside a brass cylinder which the beta particles from source can not penetrate. The cylinder has a 1mm x 6mm rectangular hole on one end. The source to hole distance is 40mm, which restricts the incident angle of beta particles from the source to the silicon pad detector.

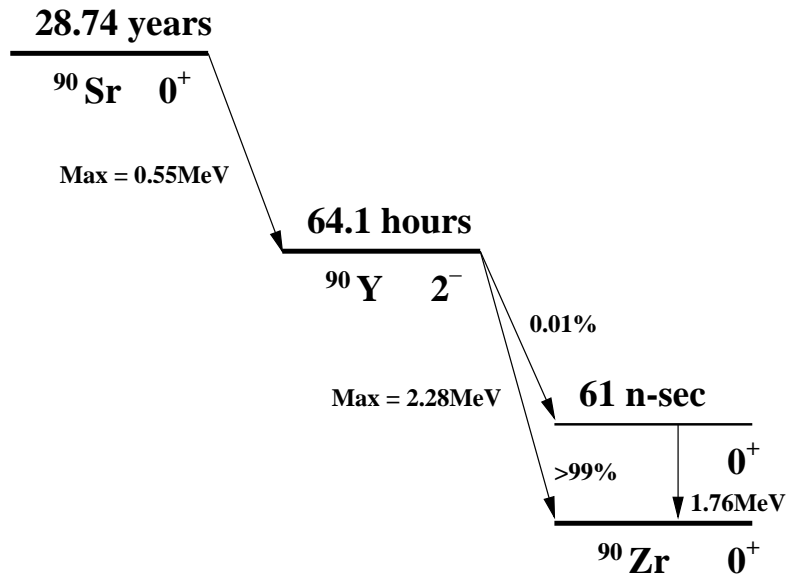


Figure 3: Decay scheme of  $^{90}\text{Sr}$ .

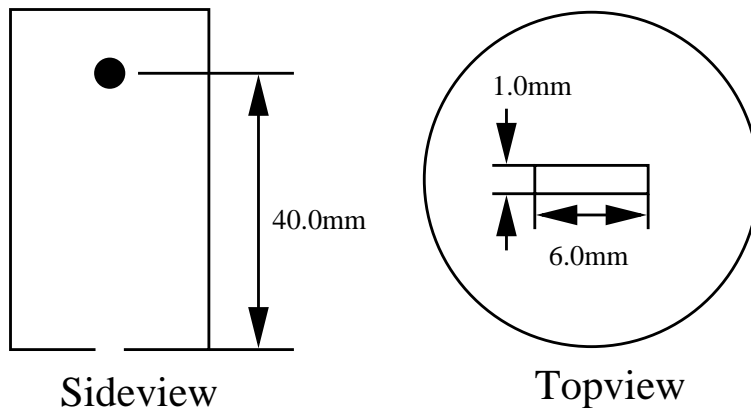


Figure 4: Source geometry: The large filled circle indicates the position of the source itself. The location of the 1 x 6mm hole at one end of the brass source container is shown.

## 2.4 Calibration

We performed two stages of calibrations. First we calibrated the external electronics which was outside the dark box. The external calibration was done with a pulse generator. We applied the same pulse to the each of the channels and measured them with the same electronics system as in the real test. We have done the two point calibration which means we applied the pulse twice per channel with different height and measured the difference between two data points in each of channels. With this calibration data we evaluated the external amplifier gain and the ADC slope of each channel. The second calibration was to measure the each Si pad detectors gain (which means the ratio of the output signal to the incident energy) and the each of the BVX pre-amplifier gains. This was done by acquiring data from all channels and comparing them to each other. The results showed that there are 10% fluctuations among channels. These fluctuations came from the combinations of Si pad detector and FEE. But we could not measure the separate fluctuations. Table 1 shows the relative gain of the each channel.

Table 1: Si pad detector+FEE gain fluctuations.

channel	relative gain
1	$1.000 \pm .003$
2	$1.050 \pm .004$
3	$0.990 \pm .004$
4	$1.020 \pm .004$
5	$1.033 \pm .004$
6	$1.003 \pm .004$
7	$0.925 \pm .004$
8	$0.951 \pm .004$

## 3 Subtraction method – using peak sensing ADC

### 3.1 Set-up

We used the all three of the trigger scintillators in this measurement. And also we included the signal from the pad detector channel which had the source pointed at it (called the “primary channel” in the discussion below) in order to exclude the severely deflected events, which means the beta particle hit a neighboring pad (not the primary channel) but scattered back into the trigger scintillators. Figure 5 shows the electronics diagram for this test. We set the threshold for each scintillator at a level just above the noise.

The coincidence unit for the scintillators used logic pulses which were 60ns wide. The coincidence between the pad channel and scintillator triggers used pulses 1  $\mu$ sec wide. We have examine the accidental coincidence rate in this setup by examining the timing pulses of pad channel and trigger channel in the digital oscilloscope. We have not observed any timing fluctuation by accidental coincidence. We have checked it later in the histogram we have taken. Figure 7 shows no tails in the primary channel. A tail in the higher energy region would be expected if there was considerable accidental coincidence by low energy beta particles. This corresponded tp our estimation of accidental coincidence rate  $1/\tau A \epsilon$  of the order of  $10^{-4}$ .

We used a pulse shaping amplifier to shape the pad detector signal and used a peak sensing ADC to digitize the pulse height of the each channel of pad detector. We connected 4 channels at one time including the channel which had the source pointed at it (the primary channel) and three of its neighbors. We made a data event set with four pad detector ADC channels and three channels of the scintillator ADCs. We used charge sensing ADC to measure trigger scintillator spectra.

In this measurement, we pointed the beta source to a selected channel of the pad detector and took ADC data of this channel and the neighboring channels. Then in the same condition we removed the pad detector from the beta source and took the background data triggered by the source and scintillators alone. The mean ADC values for the former data had contributions from the source and background including electronic noise. The second contained only the background and noise. So, when we subtract the means ADC values of the latter from the former, only the source contribution should remain. If the channels neighboring the primary channel were not hit by a real beta particle, we should get a pure crosstalk results from this measurement. In this subtraction method, we dealt with the mean value rather than bin-by-bin subtraction. The former was straightforward and caused less statistical error than the latter.

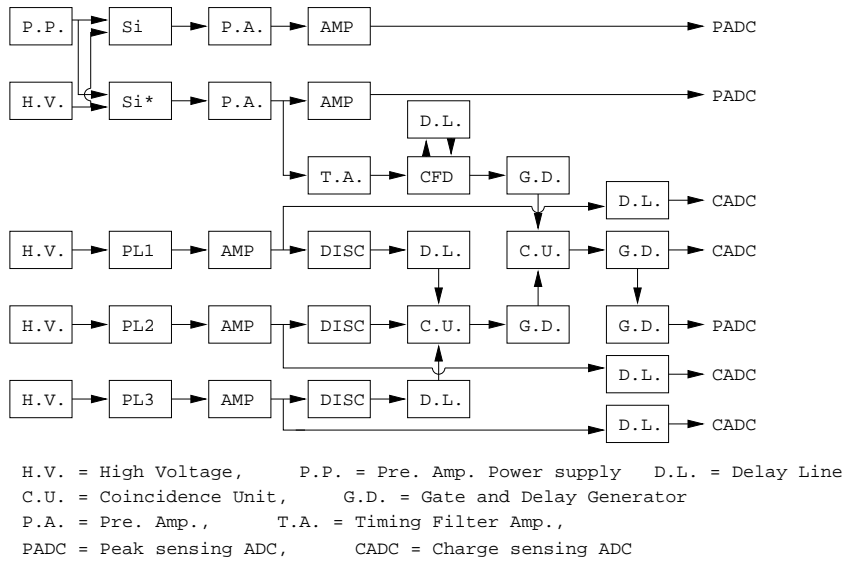


Figure 5: Electronics for the measurements using peak sensing ADC.

### 3.2 Simulation

We performed a Monte Carlo simulation using the geant code to estimate the crosstalk caused by the scattering of beta particles. We generated the beta particle energy according to the decay scheme of  $^{90}\text{Sr}$  in the figure 3. The small branching ratio to the excited state of  $^{90}\text{Zr}$  was included in this simulation. We generated flat energy distributions from 0 to their maxima beta energy instead real beta decay distribution in both  $^{90}\text{Sr}$  and  $^{90}\text{Y}$ . As shown in figure 6, the low energy beta particles like those from the  $^{90}\text{Sr}$  source in our test undergo significant scattering in the experimental setup. So there could be crosstalk from a beta particle which hits the primary channel and then is deflected

to hit a neighbor channel. This mechanism requires a second large angle scattering to scatter the electron back towards the trigger scintillators.

This simulation is also used to calculate the counting efficiency of our test setup. Table 2 shows the amounts of crosstalk due to the deflection of beta particles and the counting efficiencies in two extreme case in which are the largest pads (channels 7 and 8) and the smallest pads (channels 1–3). As expected the counting efficiency was very low, and it was mainly due to the scattering of electrons, not due to the inability of the electrons to penetrate the material in the setup. The circuit board beneath the silicon, which we could not detach from the silicon, made the efficiency much worse. Fortunately there was no cross-talk caused by the deflection effects. So all the crosstalk we measured in the test was coming out of the real crosstalk from the silicon detector and the accompanying electronics.

Table 2: Simulation result 1.

	2.0mm X 2.0mm	4.5mm x 4.5mm
crosstalk (neighbor)	0.0%	0.0%
crosstalk (next neighbor)	0.0%	0.0%
efficiency	$4.5 \times 10^{-5}$	$1.6 \times 10^{-4}$

### 3.3 Results

We connected 4 channels at one time and measured them. Figure 7 is the one example of the measurement results. Here channel 6 was the primary channel and channel 7 was its neighbor. BG in this figure means the data with the source removed from the detector. We subtracted the mean ADC value without the source (BG) from that with the source, combining the calibrations with the raw values to get the crosstalk values. Table 3 shows the results of this test. The results of eight tests are summarized. The first channel in each block represents the primary channel, and next three channels are neighbor channels which are being tested for crosstalk. In each measurement, we have taken 1,000 counts with the source on and another 1,000 with the source off. As shown in table 3, when the primary pad was one of the larger pads there was about 2% crosstalk in the neighbor big channels. The exception was channel 8. When channel 8 was the primary channel, there was no crosstalk in the neighboring big channels. When the primary channel was one of the large pads, the crosstalk was zero or negative in all of the small pads – which are in a different column than the large channels. When the primary channel was one of the to the small pads, the crosstalk was zero or negative in the large pads. In this case, there was no cross talk involving the channels with small pads (1–5) which exceeded the 1% of the real signal. Figure 8 is the summary of this measurement. The numbers inside the rectangles in the pad detector represent the measured channels, and numbers outside the rectangles represent the primary channels. We called it non-zero crosstalk when the crosstalk exceeded zero more than  $2\sigma$ . From this test we knew that there is some crosstalk between pads in the same same column, but no significant crosstalk between pads in different columns.

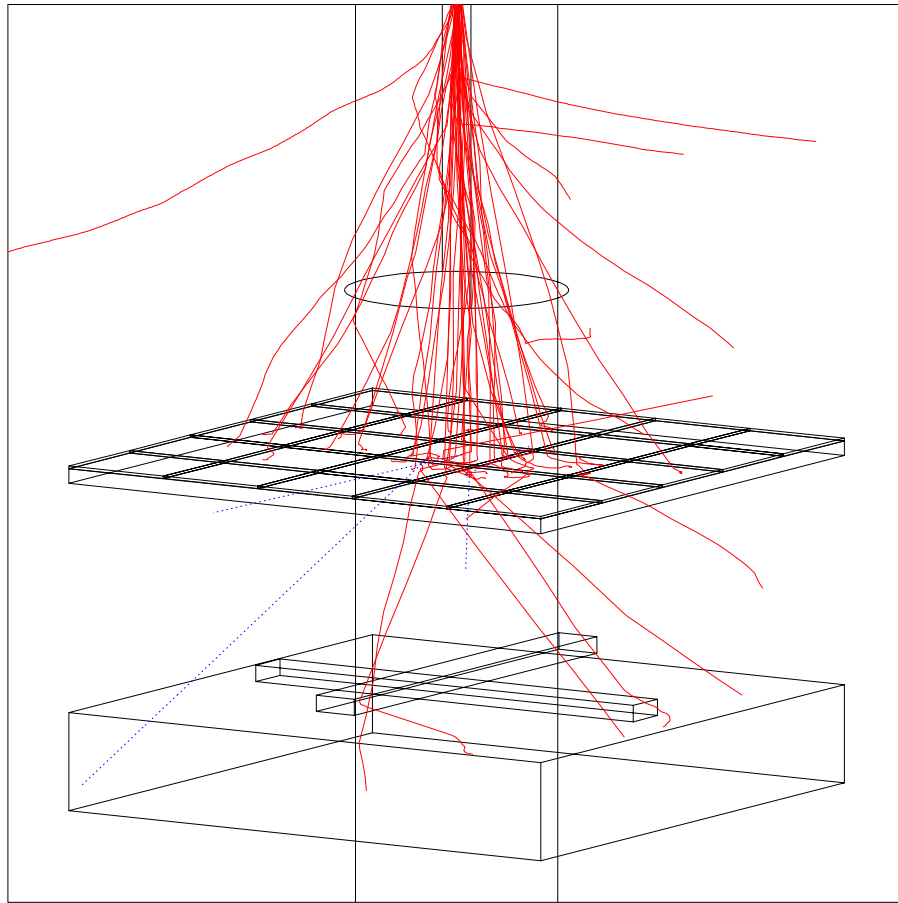


Figure 6: Deflection of electrons by the detector system: The lines starting from the top represent paths followed by the electrons. The checkboard pattern represents the pads in the Si detector. The circuit board is shown immediately below the Si detector. The small crossed rectangular solids represent the scintillating fibers and the larger block below them represents the larger trigger scintillator.

The maximum crosstalk amount did not exceed 2% of the real signal. But as you can see in the figure 8 we still could not see any clear patterns in the crosstalk. For example we could not see the direction of the crosstalk from these results. By “direction of the crosstalk,” we refer to the question of whether the crosstalk is caused in a neighbor pad (e.g. channel 8) when the signal trace for a pad (e.g. channel 6) which is hit by a particle crosses over the top of the neighbor pad, or whether the crosstalk is caused in a neighbor pad (e.g. channel 6) when its signal trace crosses over a pad which is hit (e.g. channel 8), or possibly the crosstalk could occur in both directions. Furthermore we took only 1,000 counts per each channels due to the very low counting efficiency in this set-up, and it caused larger statistical error than the other two measurements in which we have taken much more counts. One thing which could have made the measurement inaccurate is that

we used a peak sensing ADC. The ADC measured the first pulse after the opening of the gate. The test silicon pad detector + FEE system was very noisy – so the ADC could measure noise which comes early than crosstalk signal. In this case even if there was a real crosstalk signal, we could not see it. Thus the measured crosstalk values in this test could be lower than the true values. In order to check these results and see the more clear patterns of the cross-talk we performed tests using the slope method test. These tests are described in the next section.

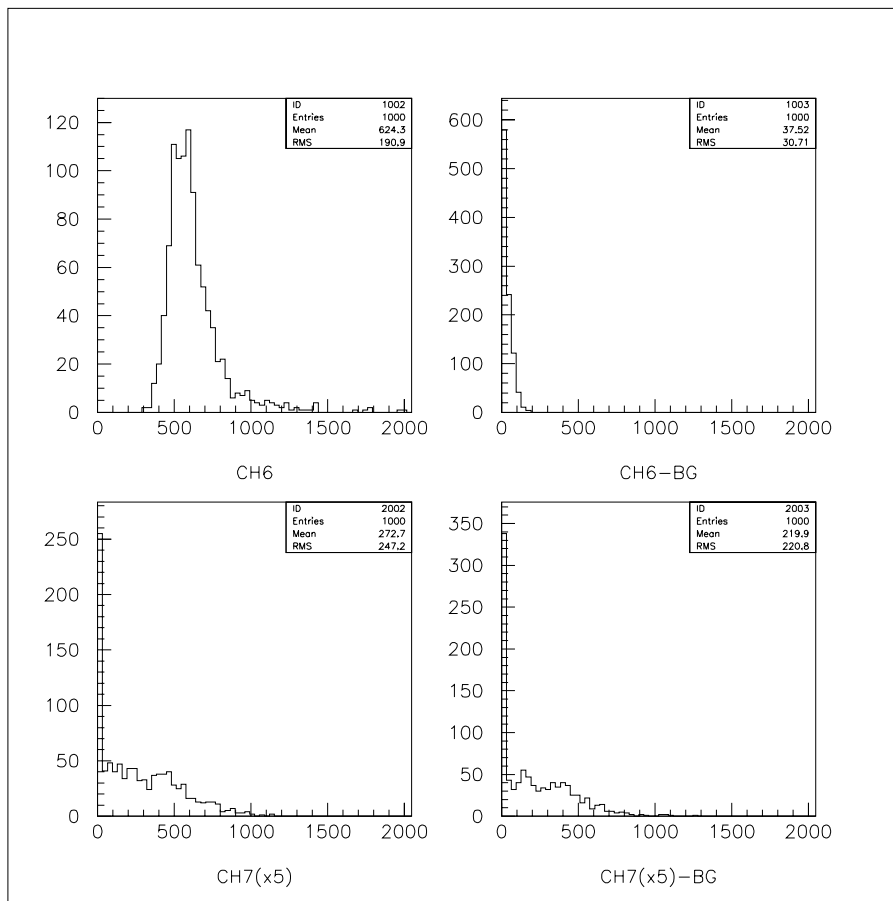


Figure 7: One example of the results 1.

## 4 Slope method - peak sensing

### 4.1 Set-up

The idea of this method was that if there was crosstalk, it would be proportional to the real signal. Thus in this method we measured the ADC data of the primary channel, cut its distribution in many energy regions, and checked the mean ADC value in each of the neighbor channels for each

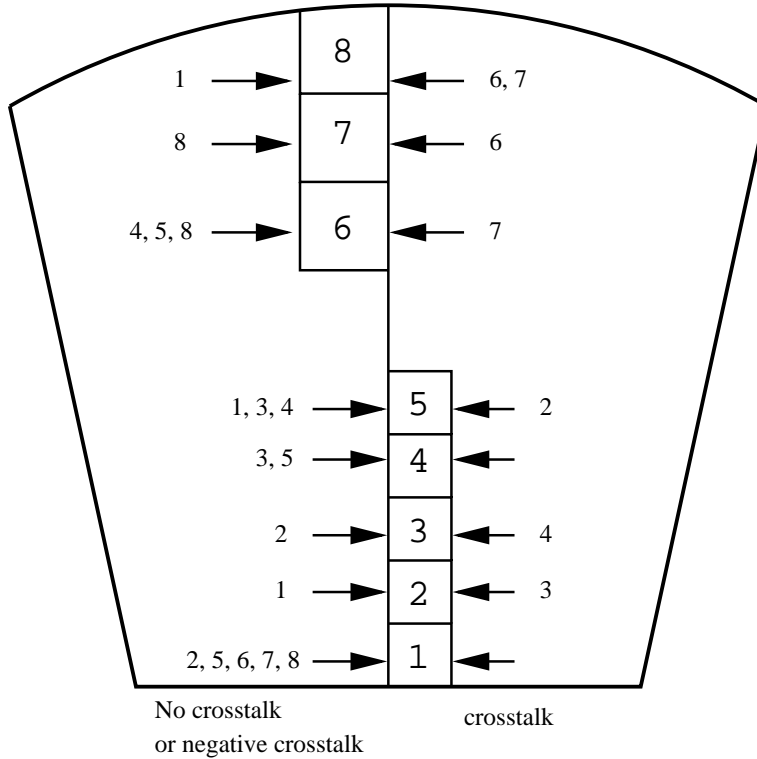


Figure 8: Summary of the results 1.

region of ADC values in the primary channel. In order to do this we needed to get a wide charge distribution in the primary pad detector channel. With three trigger scintillators on, we could get only approximately monoenergetic electrons resulting in a narrow ADC distribution. All of the trigger scintillators were turned off and only the signal from the primary pad detector channel was used as a trigger. In this case low energy beta particles could generate more charge in the pad detector, and we got a distribution in which extended to energies above the  $\approx 1$  mip signal seen with the three scintillators in the trigger. The difference can be seen by comparing the upper left histogram in figure 7 (scintillators in trigger) with the upper histogram in figure 9 (scintillators out of trigger). The electronics was the same as that of the previous subtraction method except we removed all three scintillators from the trigger. This increased the counting rate and allowed us to reduce the statistical errors.

## 4.2 Simulation

In this set-up, there was no trigger except the primary channel of pad detector itself, therefore we could expect that the scattering of electrons between the primary channel and the neighboring channels is more common. Low energy beta particles are scattered more and deposit more energy in the Si than beta particles with higher energy. Thus even if there was no real crosstalk, we could measure some crosstalk in this slope method due to scattering between pads. We performed a Monte Carlo simulation – table 4 shows the results. As you can see in the table 4, the simulation predicts crosstalk due to the scattering between nearest neighbor channels only and no crosstalk in between non-adjacent neighbors. The amount of crosstalk caused by the scattering should be

Table 3: Results 1 - Subtraction method(P.S).

channel	crosstalk (%)	Noise (%)	channel	crosstalk (%)	Noise (%)
1	–	$5.2 \pm 1$	5	–	$5.2 \pm 1$
2	$0.0 \pm 2$	–	4	$-0.7 \pm 2$	–
5	$0.2 \pm 2$	–	1	$-0.8 \pm 2$	–
8	$-0.1 \pm 2$	–	6	$-0.4 \pm 2$	–
2	–	$4.5 \pm 1$	6	–	$6.4 \pm 2$
3	$0.3 \pm 2$	–	7	$2.0 \pm 4$	–
1	$0.0 \pm 2$	–	8	$1.5 \pm 4$	–
5	$0.7 \pm 1$	–	1	$-0.4 \pm 2$	–
3	–	$4.8 \pm 1$	7	–	$7.0 \pm 2$
4	$-0.2 \pm 2$	–	6	$2.1 \pm 4$	–
5	$0.1 \pm 2$	–	8	$1.9 \pm 4$	–
2	$0.6 \pm 1$	–	1	$-0.4 \pm 2$	–
4	–	$4.9 \pm 1$	8	–	$5.2 \pm 1$
3	$0.6 \pm 2$	–	7	$0.0 \pm 2$	–
5	$0.2 \pm 2$	–	6	$0.2 \pm 2$	–
6	$-0.6 \pm 2$	–	1	$-0.1 \pm 2$	–

small, so we neglect these effects in the real measurements.

Table 4: Simulation results 2

	2.0mm X 2.0mm	4.5mm X 4.5mm
crosstalk (very neighbor)	0.14%	0.02%
crosstalk (next neighbor)	0.0%	0.0%

### 4.3 Results

Figure 9 is the one example of this measurements. The top histogram in this figure is the energy distribution in the primary channel. Comparing this histogram with figure 7 in the previous section, you can see that the energy distribution in the primary channel extended higher energies. This is an effect of removing the scintillators from the trigger. Because figure 7 shows a monoenergetic distribution in the primary channel, the wide distribution in figure 9 does not appear to be caused by the resolution of the detector and electronics. The bottom two plots in figure 9 show the crosstalk slopes. To make these two plots, we cut the ADC histogram for the primary channel (top of figure 9) into many small regions. For each of these regions in the primary channel's ADC distribution, we calculate the mean ADC value for both the primary channel and for the associated events in the neighbor channels. On the bottom two plots in figure 9, the horizontal axis represents the mean ADC values for the primary channel in each region and the vertical axis represents associated the mean ADC values in the neighbor channels. We fitted this graph with

straight line and evaluated the crosstalk. If there is crosstalk, the slope should be positive since a larger signal in the primary channel will produce a larger signal in the neighbor. The magnitude of the slope gives the cross-talk, except that the slope parameters must be divided by 5 (because the primary channel’s amplifier gain as 5 times as high as the neighbor channels) and a correction for the differences in gains between channels must be applied (see table 1). The intercept represents the noise level of each channel.

Table 5 shows the results of this test. As shown in the table, the measured crosstalk was larger than we measured with the subtraction method (see section 3). The disadvantage of a peak sensing ADC was that it converts the first coming pulse after the gate opening. It could record noise peak instead of real crosstalk peak. Moreover the crosstalk could not be superposed to noise just in phase in most cases because noise occurred randomly regardless of the crosstalk. So when we used the peak sensing ADC, the pulse height of the superposed signal was, in most cases, less than the sum of the pulse height of noise and crosstalk. This always gave us a smaller measured value of the crosstalk than the real value. Figure 10 is the summary of the results. The overall crosstalk patterns roughly corresponded to those seen with the subtraction method. In the large channels these measurements see crosstalk in “both directions” (e.g. primary channel 6 causes a signal in channel 8 and primary channel 8 also causes a signal in channel 6). But the patterns of crosstalk are still unclear in the small channels.

Table 5: Results 2 - Slope method(P.S.)

channel	crosstalk (%)	channel	crosstalk (%)
1	–	5	–
2	1.33±.04	4	0.99±.06
5	1.00±.05	1	0.80±.06
8	-0.03±.06	6	-0.20±.06
2	–	6	–
3	1.74±.05	7	2.24±.06
1	1.43±.05	8	1.92±.06
5	0.73±.03	1	-0.35±.03
3	–	7	–
4	0.96±.05	6	2.87±.05
2	0.98±.06	8	2.79±.05
8	-0.18±.06	1	-0.29±.03
4	–	8	–
3	1.26±.05	7	3.29±.05
5	1.02±.06	6	2.35±.05
6	-0.02±.06	1	-0.27±.03

## 5 Subtraction method - charge sensing

### 5.1 Set-up

As mentioned in the previous sections, the crosstalk signal could be hidden by the noise in the peak sensing ADC measurements. We replaced the peak sensing ADC with a charge sensing ADC to

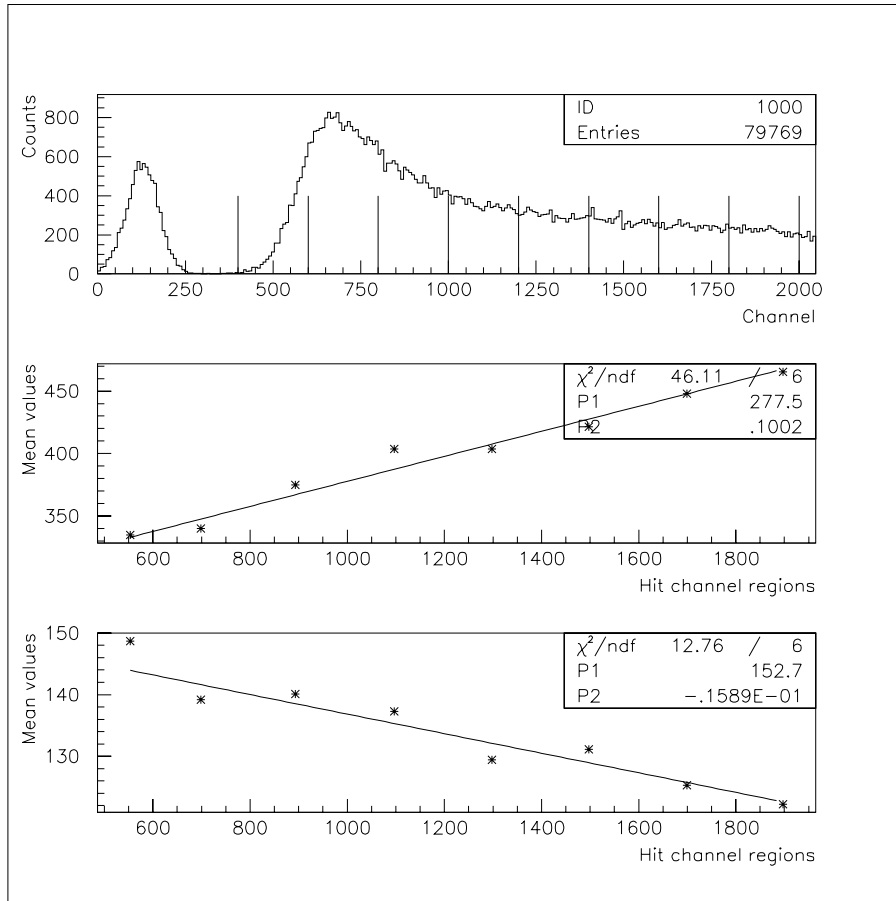


Figure 9: One example of the results 2. The abscissas of the middle and the bottom plots represent the primary channel's average pulse height in each energy region, and the ordinates of them represent the corresponding average crosstalk plus background noise pulse height in the neighboring channels.

eliminate this potential problem. We also removed the fiber scintillators from the trigger and made a trigger with the thick scintillator and the hit channel of pad detector. This increased the count rate and therefore reduced the statistical uncertainties. We also replaced the pulse shaping amplifier with an amplifier which does not do pulse shaping. Figure 11 shows the electronics diagram for this measurement. In this measurement we took data from eight channels simultaneously. The data analysis method is same as the of the subtraction method with the peak sensing ADC (see section 3).

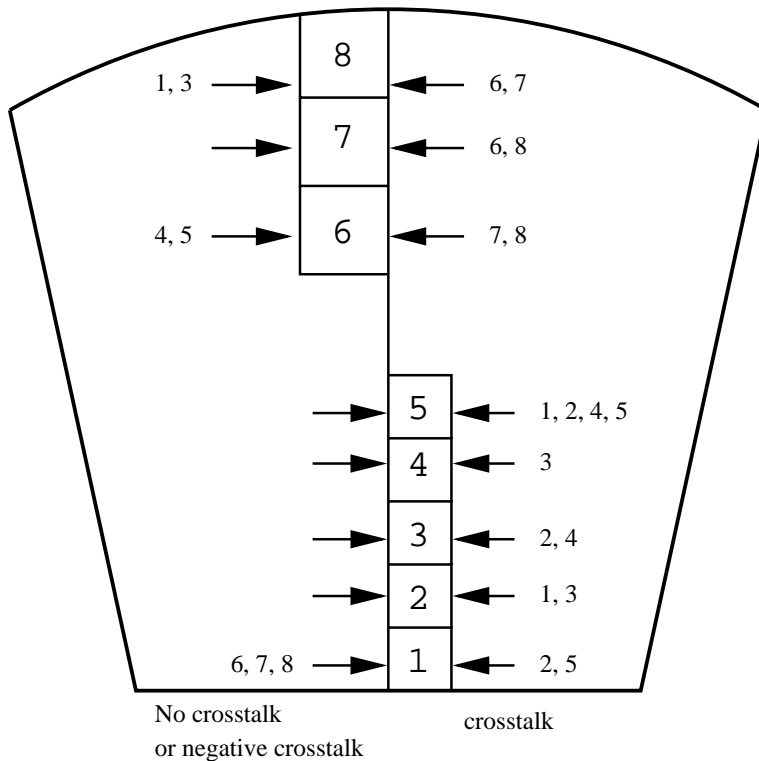


Figure 10: Summary of the results 2.

## 5.2 Simulation

By removing the fiber scintillators from the trigger to increase the counting efficiency, we lost our precise definition of the direction of the incident beta particle. Therefore, another simulation was needed to check the validity of this test set-up. The method of simulation was the same as that of the measurement with the peak sensing ADC. Table 6 shows the results of this simulation. As we expected the counting efficiency was increased more than factor of 100. But there was some crosstalk due to the scattering of the beta particles between neighboring channels. Fortunately the amount of the crosstalk due to the scattering is small – as shown in the Table 6. The simulations show that the scattering-induced “crosstalk” affects only the nearest neighbor channel. Any crosstalk above the simulation value should be the result of “real” crosstalk.

Table 6: Simulation results 3

	2.0mm x 2.0mm	4.5mm x 4.5mm
crosstalk (very neighbor)	0.19%	0.09%
crosstalk (next neighbor)	0.0%	0.0%
efficiency	$6.2 \times 10^{-3}$	$1.9 \times 10^{-2}$

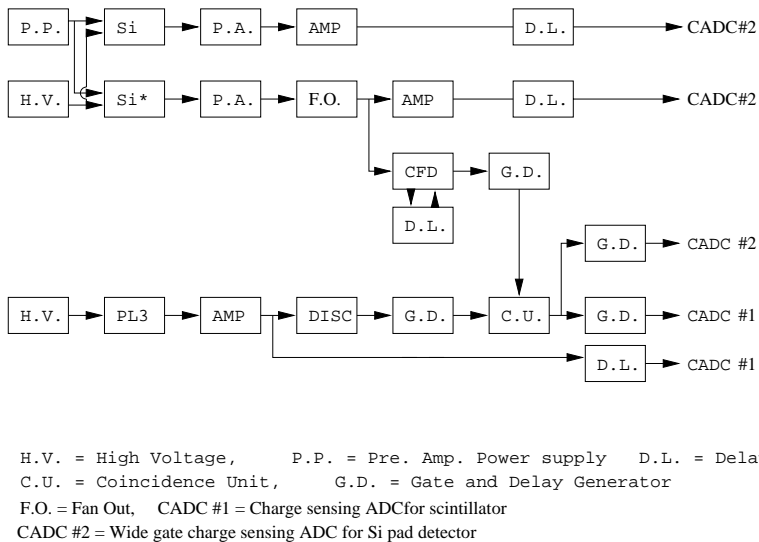


Figure 11: Electronics for the measurements using charge sensing ADC.

### 5.3 Results

In this test we simultaneously connected and measured results for each of the 8 channels which had been wirebonded. The data were analyzed with the subtraction method (see section 3), except this time a charge sensing ADC was used. Figure 12 shows one example of the results. In this measurement we set the ADC gate wide enough to accept all the crosstalk signals at the sacrifice of increasing noise levels. Also we took 20,000 counts per channel, which reduced the statistical error significantly compared to the previous subtraction measurement using peak sensing ADC (section 3).

Table 7 shows the results of this test. For four (of eight total) different primary channels, figure 12 summarizes the results in table 7. In each part of the figure, the arrow marks the primary channel (i.e. the channel which is in the trigger and has the source pointing at it). Figure 14 summarizes summary of the results in a different format. These measurements show clear patterns in the crosstalk. The direction of the crosstalk is bi-directional — any pair of pads for which the readout trace of one pad crosses the other pad exhibits crosstalk. When a large pad was the primary channel, the crosstalk was about 2.6% in the neighboring large channels and -0.5% in the small channels (which are in the other column). When the primary channel was one of the small pads, there was about 1.7% crosstalk in the other small channels and 0.2% crosstalk in the large channels. The exception to this pattern is channel 2. When the primary channel was channel 2, the crosstalk was  $\approx 2.8\%$  in the other small pads and  $\approx 1.4\%$  in the large pads.

## 6 Summary and Discussion

In these beta test measurements, we found that there was no cross talk which exceeded the 3% of the real signal, that means the double metal silicon pad detector can be used as the PHENIX MVD detector component. The major crosstalk occurred between and pair of pads in the same column. The amount of the crosstalk between the small channels was about 2/3 of that between

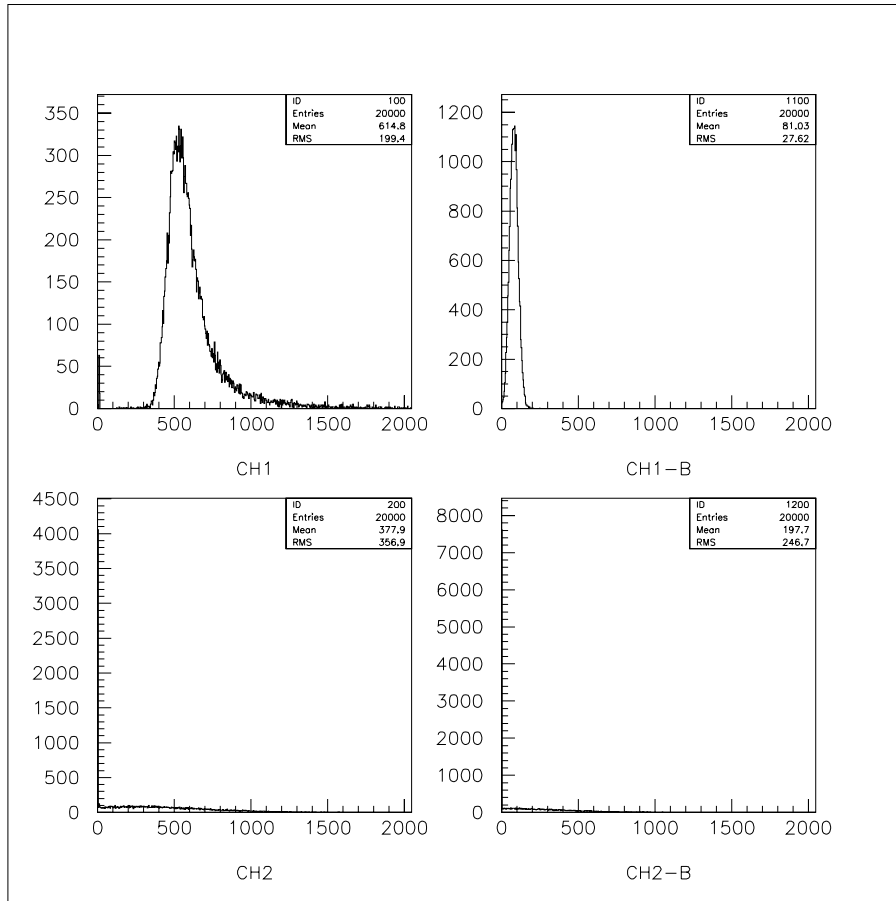


Figure 12: One example of the results 3.

large channels. In most cases, there was much less crosstalk between pads in different columns. occurred in other columns. There was some small positive crosstalk observed in the large channels when the primary channel was one of the small channels. There was a small amount of negative crosstalk in the small channels when the primary channel was one of the the large pads. We are not sure whether this minor crosstalk came from the detector itself or from the electronics.

We also noted that in order to get a good results we needed to integrate all the signal from the detector system, thus it was useful to use a charge integrating ADC in this test. The full trigger was necessary to define the incident angle of beta particle and this reduced the crosstalk by the beta particle scattering. But this factor was found to be less important than the factor from the statistical error due to low counting rate. Our simulations showed that only a rough trigger like big scintillator trigger in our case should be good enough to give us a good results. Thus it was more efficient to increase the counting efficiency by simplification of the trigger in order to get a

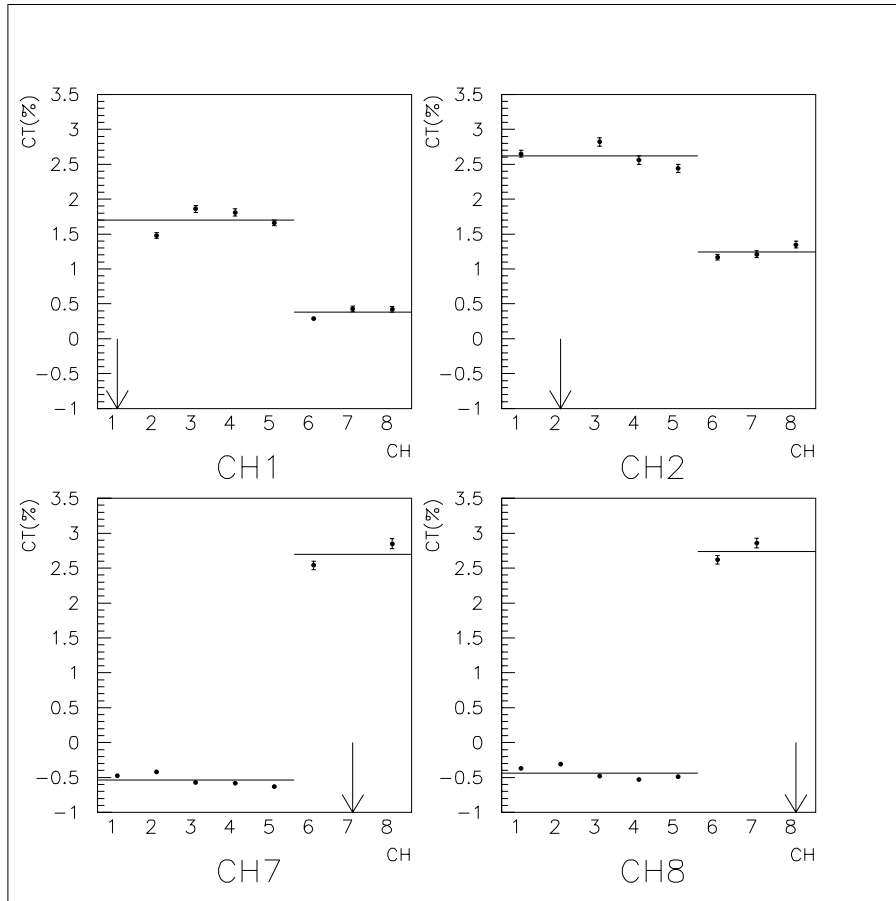


Figure 13: Some graphs of the results 3.

more reliable results. But the difference between the results using the full trigger and the results using the simplified trigger was beyond the statistical error. The reason for this difference is not clear yet. We have been trying to understand the effects of the full trigger.

For the simple cases with only one hit on the detector, the small amount of crosstalk seen in these studies should not cause any major problems. However, complicated patterns of minor crosstalk are seen in our measurements. In events with high multiplicity, the overall crosstalk patterns would be very complicated. In order to understand the patterns fully, we need to do tests with more channels connected.

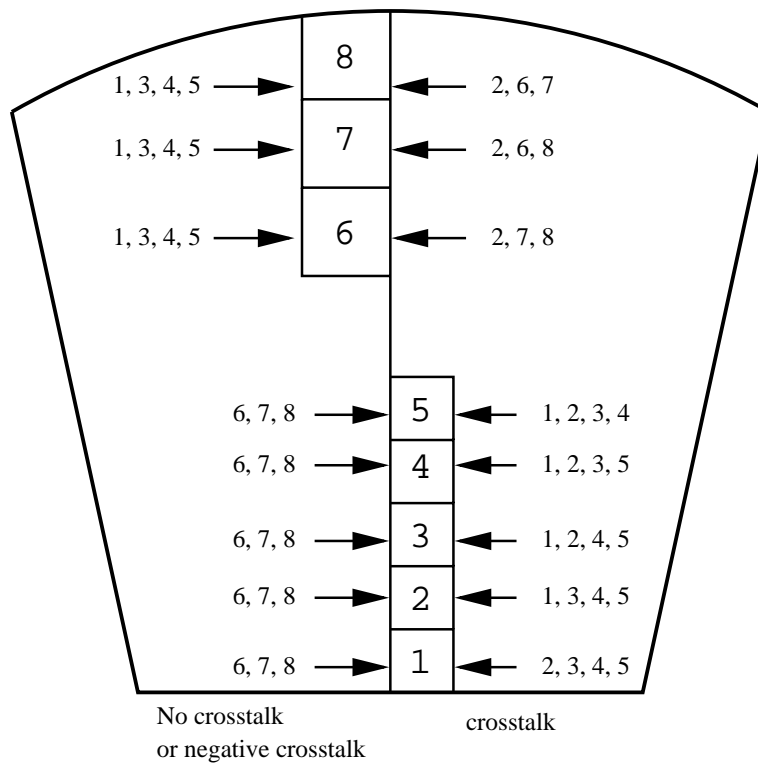


Figure 14: Summary of the results 3.

Table 7: Results 3 - Subtraction method(C.S.)

channel	crosstalk (%)	Noise (%)	crosstalk (%)	Noise (%)
1	–	15.17±.05	1.69±.04	–
2	1.48±.04	–	1.73±.05	–
3	1.86±.05	–	1.77±.04	–
4	1.81±.05	–	1.60±.05	–
5	1.66±.04	–	–	14.67±.05
6	0.29±.03	–	0.24±.03	–
7	0.43±.04	–	0.23±.04	–
8	0.42±.04	–	0.16±.04	–
1	2.65±.05	–	-0.58±.03	–
2	–	14.38±.05	-0.50±.02	–
3	2.82±.06	–	-0.68±.03	–
4	2.56±.06	–	-0.68±.03	–
5	2.44±.06	–	-0.70±.03	–
6	1.17±.04	–	–	15.09±.05
7	1.21±.05	–	2.45±.06	–
8	1.35±.05	–	2.50±.07	–
1	1.64±.06	–	-0.47±.03	–
2	1.80±.05	–	-0.42±.03	–
3	–	15.34±.06	-0.57±.03	–
4	1.73±.05	–	-0.58±.03	–
5	1.60±.04	–	-0.63±.03	–
6	0.24±.03	–	2.54±.06	–
7	0.15±.04	–	–	16.38±.06
8	0.26±.04	–	2.85±.07	–
1	1.70±.04	–	-0.37±.02	–
2	1.73±.05	–	-0.31±.03	–
3	1.92±.05	–	-0.48±.03	–
4	–	14.82±.05	-0.53±.03	–
5	1.49±.04	–	-0.49±.03	–
6	0.16±.03	–	2.62±.06	–
7	0.17±.04	–	2.86±.07	–
8	0.17±.04	–	–	16.01±.06